

## Comparative Quantum Chemical Study of Stabilization Energies of $\text{Zn}^{2+}$ Ions in Different Zeolite Structures

Alexander A. Shubin\* and Georgii M. Zhidomirov

Boriskov Institute of Catalysis, Prosp. Akad. Lavrentieva 5, Novosibirsk 630090, Russia

Alexei L. Yakovlev\* and Rutger A. van Santen

Schuit Institute of Catalysis, Eindhoven University of Technology, P.O. Box 513, 5600 MB, Eindhoven, The Netherlands

Received: October 31, 2000; In Final Form: February 28, 2001

Cluster model quantum chemical calculations have been performed to compare stabilization energies ( $E_{\text{st}}$ ) of  $\text{Zn}^{2+}$  ions in four-, five-, and six-membered zeolitic rings.  $E_{\text{st}}$  was evaluated as energy of the reaction  $\text{Zn}^{2+}/\text{Z} + \text{H}_2 \Rightarrow 2\text{H}^+/\text{Z} + \text{Zn}^0$ . It was found that  $E_{\text{st}}$  substantially decreases in the series six-, five-, and four-membered ring, and this trend is essential to the understanding of the comparative adsorption ability and reactivity of  $\text{Zn}^{2+}$  in cationic sites of different zeolites. This conclusion was proved in calculations of the heterolytic dissociation of ethane. The molecular structure of active sites in  $\text{ZnHY}$  and  $\text{ZnHZSM-5}$  zeolites and the question of the stability of small intrazeolite zinc oxide species are discussed.

### Introduction

Recently, Zn containing zeolites, and especially  $\text{ZnHZSM-5}$ , attracted much attention because of their catalytic activity in dehydrogenation of light alkanes and aromatization of hydrocarbons.<sup>1,2</sup> Considerable effort was devoted to clarifying the structure of possible  $\text{Zn}^{2+}$ -ion oxide species in these systems and to the determination of their catalytically active forms.<sup>3–5</sup> Although Zn-containing faujasites appeared to be not as efficient as  $\text{ZnHZSM-5}$  in dehydrogenation and aromatization of alkanes, they also attract substantial attention in the literature.<sup>6–10</sup> One of the questions common for both types of zeolites is the stability of small intrazeolite oxide particles. These species have unusual physical and chemical (catalytic) properties.<sup>11,12</sup> Unfortunately, because of the complexity of the systems under study, many problems concerning the state and reactivity of zinc ion species in these zeolite systems remain. Thus, there is no definite explanation of the drastic difference between  $\text{ZnZSM-5}$  and  $\text{ZnHY}$  in alkane dehydrogenation ability. Molecular modeling of proposed chemical structures of active sites for high-silica zeolites encounters some difficulties; the structure of intermediates of the thermal treatment and interaction with water, hydrogen, and alkane molecules is unclear. For instance, difficulties in the observation of the IR band of  $\text{ZnOH}$  hydroxyl groups in both kinds of zinc zeolites<sup>10,13</sup> demand the structural interpretation.

Different suggestions have been made concerning the role of the zinc component of the catalyst in the catalytic process.<sup>4</sup> Because a theoretical study of molecular models of different locations of metal cations in zeolite structures can help to better understand chemical properties of the Zn form of a zeolite, we have performed cluster model quantum chemical calculations

of  $\text{Zn}^{2+}$  ions in four-, five-, and six-membered zeolite rings. It is well-known that metal cations prefer sites with high coordination to the framework oxygen atoms. For instance, in faujasites, these are  $\text{S}_\text{I}$ ,  $\text{S}_\text{I}'$ ,  $\text{S}_\text{II}$ , and  $\text{S}_\text{II}'$  (six-membered rings) and  $\text{S}_\text{III}$  and  $\text{S}_\text{III}'$  (four-membered rings) sites. Significantly less is known about cationic positions in ZSM-5 zeolites, and only recently, a classification of the positions was attempted.<sup>14</sup> The main fragments of the ZSM-5 framework are five-membered rings, but also four-membered rings do exist in the structure as well as effective six-membered rings. The latter are formed by two interconnected five or six rings. Previously, such models for cationic sites of ZSM-5 zeolites have been theoretically considered: for the  $\text{Cu}^+$  ion (four-membered ring with one Al atom),<sup>15</sup> for the  $\text{Cu}^{2+}$  ion (six- and five-membered rings with two Al atoms),<sup>16</sup> and for the  $\text{Zn}^{2+}$  ion (four-membered ring with two Al atoms).<sup>17</sup> The applicability of these models depends on the Si/Al ratio of a zeolite.

The primary aim of our investigation is the comparison of the stability of  $\text{Zn}^{2+}$  ions in six-, five-, and four-membered zeolitic rings. We define this quantity as the energy of transition to the H form of these rings. This characteristic is rather suitable for qualitative consideration of different zeolite systems and for understanding their reactivity. It is actually a key factor, which determines the stability of oxide nanoclusters in zeolite pore materials, because one of the main questions here is their preferable formation compared to conventional ion exchange.

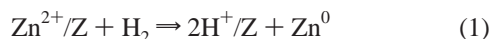
We have chosen the heterolytic dissociation of an ethane molecule for comparison of catalytic activity of  $\text{Zn}^{2+}$  ions in four-, five-, and six-membered zeolitic rings according to the suggestion that metal cations are involved in alkane dehydrogenation reaction.<sup>18</sup> Up to now, the nature of active sites in  $\text{ZnHZSM-5}$  zeolites is still a subject of discussion.<sup>3,5,13</sup> In particular, some other probable structures of the active sites have been suggested.<sup>3,5</sup> Small zinc oxide clusters,<sup>13</sup> binuclear ( $\text{Zn}-\text{O}-\text{Zn}$ )<sup>2+</sup> moieties,<sup>3</sup> and  $\text{Zn}^+-\text{OSi}\equiv$  and  $\equiv\text{SiO}-\text{Zn}-\text{OSi}\equiv$

\* To whom correspondence should be addressed. Fax: +7 (3832) 343056. E-mail: A.A.Shubin@catalysis.nsk.su. E-mail: Zhi@catalysis.nsk.su. Fax: +31 (40) 2455054. E-mail: A.L.Yakovlev@tue.nl. E-mail: R. A.v.Santen@tue.nl.

species modeling defect sites should be mentioned.<sup>5</sup> We shall discuss these types of active sites in our subsequent communications.

### Computation Details

Cluster model quantum chemical calculations have been performed to compare stabilization energies ( $E_{\text{st}}$ ) of  $\text{Zn}^{2+}$  ions in different zeolitic rings.  $\text{ZnSi}_4\text{Al}_2\text{O}_6\text{H}^*_{12}$ ,  $\text{ZnSi}_3\text{Al}_2\text{O}_5\text{H}^*_{10}$ , and  $\text{ZnSi}_2\text{Al}_2\text{O}_4\text{H}^*_{8}$  clusters were chosen as molecular models of cationic sites for  $\text{Zn}^{2+}$  ion in six-, five-, and four-membered zeolitic rings, respectively. Here  $\text{H}^*$  are boundary atoms saturating dangling bonds of the Si and Al atoms in the structure. The stabilization energy ( $E_{\text{st}}$ ) of the  $\text{Zn}^{2+}$  ion was determined as energy change in the reaction:



Taking into account the energy of possible condensation of Zn atoms into small Zn metallic clusters, we have calculated the energy of formation of small  $\text{Zn}_2$  and  $\text{Zn}_4$  clusters with different basis sets up to 6-31G\*. In all cases, the “heat of condensation” was low for these particular small clusters. A maximum value of 3.2 kcal/mol (per mole of Zn) was obtained for  $\text{Zn}_4$  using density-functional theory (DFT) with gradient-corrected Becke exchange<sup>19</sup> and Pedrew correlation<sup>20</sup> functionals and the 6-31G\* basis set.

The H forms of the zeolitic rings were modeled by the  $\text{Si}_4\text{Al}_2\text{O}_6\text{H}_2\text{H}^*_{12}$ ,  $\text{Si}_3\text{Al}_2\text{O}_5\text{H}_2\text{H}^*_{10}$ , and  $\text{Si}_2\text{Al}_2\text{O}_4\text{H}_2\text{H}^*_{8}$  clusters calculated in a similar manner. Final structures of heterolytic dissociation of the ethane molecule into  $\text{C}_2\text{H}_5^-$  and  $\text{H}^+$  on  $\text{Zn}^{2+}/\text{Z}$  for all of the above-mentioned ring models were found, as well as energies of the ethylene molecule elimination. Most calculations were performed at the SCF Hartree–Fock (HF) level with LANL2DZ basis set using Gaussian92 and Gaussian98 programs.<sup>21</sup> For optimized geometries, single-point calculations were also performed using DFT with gradient-corrected Becke exchange and Pedrew correlation functionals. To verify the most important predictions of this work, additional computations were performed for some key structures with the use of all-electron basis sets for the Zn atom<sup>22</sup> and 3-21G\* for other elements instead of a LANL2DZ pseudopotential. It was verified that calculations at the LANL2DZ level are sufficient for the purposes of the current study. For example, the differences in  $E_{\text{st}}$  for six ring and in the heterolytic dissociation energy of  $\text{H}_2$  on  $\text{Zn}^{2+}$  ion in the six ring at HF level do not exceed 6–8 kcal/mol for different basis sets. Because our aim is a semiquantitative comparison, we did not make corrections for zero-point energies.

One of the key questions of cluster modeling of the zeolite fragments is the choice of the cluster geometry. If one aims at an “averaged” comparison of different cationic sites for  $\text{Zn}^{2+}/\text{Z}$ , full geometry optimization of the clusters is chosen. In real zeolites, the geometry of the rings is different from the completely optimized structure. At the same time, the geometry of similar cationic positions is slightly different for different four-, five-, and six-member rings in the same zeolite structure. This has an influence on the  $E_{\text{st}}$ . We can illustrate this on the example of six-membered rings. Full geometry optimization for  $\text{Zn}^{2+}/\text{Z}$ , where Al atoms are in positions opposite to each other in the ring, leads to a planar structure of the active center (Zn and T atoms are in one plane) and the four-coordinated  $\text{Zn}^{2+}$  ion. Structural characterization<sup>23</sup> indicates that the  $\text{Zn}^{2+}$  ion in  $\text{S}_{\text{II}}$  sites of faujasites prefers the three-coordinated structure; however, this conclusion was drawn without specific determi-

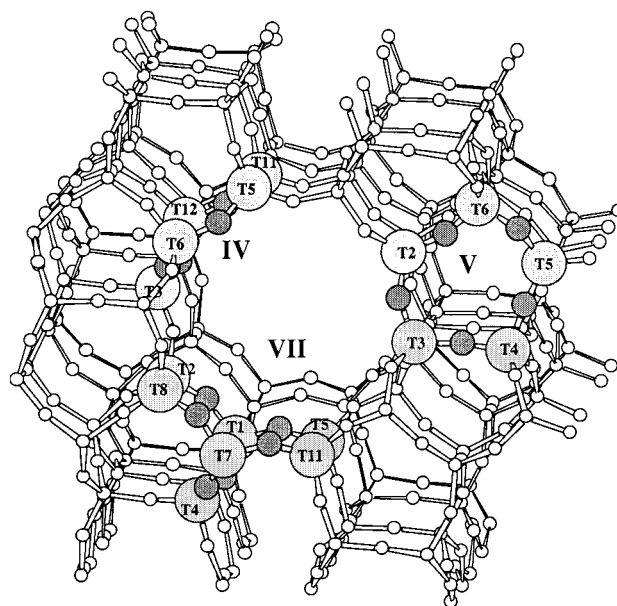


**Figure 1.** Location of the considered models of ZSM-5 zeolite in its crystal lattice: a five ring in the straight channel (IV), a five ring in the sinusoidal channel (V), and an  $\alpha$  site (VII).

nation of the position of Al ions in the ring. In principle, there are two possibilities to place two Al ions in a six-membered ring. This can result in somewhat different coordination surrounding for the  $\text{Zn}^{2+}$  ion. A more definitive conclusion can be made for the ZnA zeolite with its mostly homogeneous distribution of Si and Al atoms in the lattice. A three-coordinated structure for  $\text{Zn}^{2+}$  ion in  $\text{S}_{\text{II}}$  site was found in the single-crystal XRD study of the ZnA zeolite; at the same time, a strong trend of the  $\text{Zn}^{2+}$  ion to form an additional bond with nonframework oxygen was mentioned.<sup>24</sup> This was confirmed by an X-ray absorption spectroscopy study.<sup>25</sup> The appearance of the three-coordinated structure is not associated with intrinsic properties of the zinc ion (indeed, it strongly prefers the four-coordinated structure to the three-coordinated one) but with the specific deformation of the six-membered rings of faujasite  $\text{S}_{\text{II}}$  site. In cluster calculations, such a deformation can be taken into account by imposing special restrictions on the optimization of positions of boundary  $\text{H}^*$  atoms.<sup>26</sup> We have carried out such a calculation for the  $\text{ZnSi}_4\text{Al}_2\text{O}_6\text{H}^*_{12}$  cluster with opposite position of Al ions in the ring using a similar procedure for a series of restricted geometry optimizations. At the first step of the optimization procedure, the entire frame  $\text{Si}_4\text{Al}_2\text{O}_6$  was fixed according to experimental X-ray diffraction data.<sup>27</sup> Only Si– $\text{H}^*$  and Al– $\text{H}^*$  bond distances were optimized, whereas the orientation of  $\text{H}^*$  hydrogen atoms was kept fixed toward the corresponding oxygen ions of the crystal. The  $\text{Zn}^{2+}$  ion was allowed to move freely in the structure. In the second step, optimization was performed with fixed positions of  $\text{H}^*$  atoms. The same fixed positions of  $\text{H}^*$  atoms were used further for the restricted geometry optimizations of H forms and other structures. Similar restricted geometry optimizations were performed also in order to model “real” five-membered rings and  $\alpha$ -site position in the ZSM-5 zeolite, on the basis of the crystal structure found in XRD study.<sup>28</sup> These sites are shown in Figure 1 and the details are described in Table 1. It is noteworthy that, in contrast to a six-membered ring in faujasite, taking the real geometry of the rings in the ZSM-5 zeolite lattice into account substantially decreases stabilization energies of  $\text{Zn}^{2+}$  in cationic positions compared to full geometry optimization (see Table 1).

**TABLE 1: Calculated Energies (kcal/mol) of the Reactions  $\text{Zn}^{2+}/\text{Z} + \text{H}_2 \rightarrow (\text{2H}^+)/\text{Z} + \text{Zn}^0$  ( $E_{\text{st}}$ );  $\text{Zn}^{2+}/\text{Z} + \text{C}_2\text{H}_6 \rightarrow (\text{ZnC}_2\text{H}_5^+ + \text{H}^+)/\text{Z}$  ( $E_{\text{ads}}(\text{C}_2\text{H}_6)$ );  $(\text{ZnC}_2\text{H}_5^+ + \text{H}^+)/\text{Z} \rightarrow (\text{ZnH}^+ + \text{H}^+)/\text{Z} + \text{C}_2\text{H}_4$  ( $E_{\text{des}}(\text{C}_2\text{H}_4)$ ); and  $(\text{ZnH}^+ + \text{H}^+)/\text{Z} \rightarrow \text{Zn}^{2+}/\text{Z} + \text{H}_2$  ( $E_{\text{des}}(\text{H}_2)$ ) for Different Zeolitic Rings (Energy is Positive for Endothermic Reactions)**

structure	$E_{\text{st}}$	$E_{\text{ads}}(\text{C}_2\text{H}_6)$	$E_{\text{des}}(\text{C}_2\text{H}_4)$	$E_{\text{des}}(\text{H}_2)$	comments
<b>I</b> six ring (Figure 2a), four-coordinated $\text{Zn}^{2+}$	59.7	46.5	20.6	-24.1	(a) Full geometry optimization (b) Four-coordinated Zn in $(\text{ZnH}^+ + \text{H}^+)/\text{Z}$ ; three-coordinated Zn in $(\text{ZnC}_2\text{H}_5^+ + \text{H}^+)/\text{Z}$
<b>II</b> six ring in faujasite (Figure 3a), three-coordinated $\text{Zn}^{2+}$	72.9	37.5	29.6	-24.1	(a) Geometry optimization with imposed restrictions according to $S_{\text{II}}$ cationic position in faujasites (b) Four-coordinated Zn in $(\text{ZnH}^+ + \text{H}^+)/\text{Z}$ ; three-coordinated Zn in $(\text{ZnC}_2\text{H}_5^+ + \text{H}^+)/\text{Z}$
<b>III</b> five ring (Figure 4a), four-coordinated $\text{Zn}^{2+}$	47.2	28.3	28.7	-14.0	(a) Full geometry optimization (b) Four-coordinated Zn in $(\text{ZnH}^+ + \text{H}^+)/\text{Z}$ and $(\text{ZnC}_2\text{H}_5^+ + \text{H}^+)/\text{Z}$
<b>IV</b> five ring in the straight channel of ZSM-5 (Figure 5a), four-coordinated $\text{Zn}^{2+}$	25.5	14.2	29.6	-0.8	(a) Geometry optimization with imposed restrictions according to five-membered ring formed by T3, T5, T6, T11, and T12 positions in the straight channel of ZSM-5. Aluminum atoms are in T5 and T12 positions. Hydrogen atoms in H form are near O5 and O11. (b) Four-coordinated Zn in $(\text{ZnH}^+ + \text{H}^+)/\text{Z}$ and $(\text{ZnC}_2\text{H}_5^+ + \text{H}^+)/\text{Z}$ (c) There is a hydrogen atom near O11 for all forms except $\text{Zn}^{2+}/\text{Z}$
<b>V</b> five ring in the sinusoidal channel of ZSM-5 (Figure 6a), four-coordinated $\text{Zn}^{2+}$	35.7	12.9	29.1	1.1	(a) Geometry optimization with imposed restrictions according to five-membered ring formed by T2, T3, T4, T5, and T6 positions in the sinusoidal channel of ZSM-5. Aluminum atoms are in T3 and T5 positions. Hydrogen atoms in H form are near O2 and O5. (b) Five-coordinated Zn in $(\text{ZnH}^+ + \text{H}^+)/\text{Z}$ and $(\text{ZnC}_2\text{H}_5^+ + \text{H}^+)/\text{Z}$ (c) There is hydrogen atom near O5 for all forms except $\text{Zn}^{2+}/\text{Z}$
<b>VI</b> four ring (Figure 7a), four-coordinated $\text{Zn}^{2+}$	16.3	8.7	30.2	4.1	(a) Full geometry optimization (b) Four-coordinated Zn in $(\text{ZnH}^+ + \text{H}^+)/\text{Z}$ and $(\text{ZnC}_2\text{H}_5^+ + \text{H}^+)/\text{Z}$
<b>VII</b> $\alpha$ site in ZSM-5 (effective six ring) (Figure 8a), four-coordinated $\text{Zn}^{2+}$	19.4	9.9	31.9	1.2	(a) Geometry optimization with imposed restrictions according to $\alpha$ site formed in the straight channel by T1, T2, T5, T7, T8, T11, and T4 positions. Aluminum atoms are in T2 and T11 positions. Hydrogen atoms in H form are near O1 and O22. (b) Three-coordinated Zn in $(\text{ZnH}^+ + \text{H}^+)/\text{Z}$ and $(\text{ZnC}_2\text{H}_5^+ + \text{H}^+)/\text{Z}$ (c) There is a hydrogen atom near O1 for all forms except $\text{Zn}^{2+}/\text{Z}$

Certainly, the adopted scheme of calculations using the experimental X-ray diffraction data and subsequent restricted geometry optimization (with fixed boundary  $\text{H}^*$  atoms) is a rather artificial method, and it can lead to some inaccuracy. The most important factors contributing to the inaccuracy are the following:

(1) The use of “average” experimental X-ray diffraction structure, because there is no possibility to know from the experiment at which positions of the ring Si atoms are isomorphously substituted by Al. This can result in some artificial tensions and deformations in the vicinity of Al atoms.

(2) Basis set dependence of the difference between experimental and optimized bond lengths and angles.

(3) The use of fixed positions of boundary atoms  $\text{H}^*$  obtained from the Zn form of the ring may influence the calculated value of  $E_{\text{st}}$ , because this can result in significant stress when such positions are used for the corresponding H form.

Nevertheless, this scheme can help us to roughly estimate the role of the real lattice geometry of zeolite rings. At the same

time, to trace the influence of the applied geometrical constraints on the stabilization of  $\text{Zn}^{2+}$  ions, we performed full geometry optimization calculations of clusters imitating  $\text{Zn}^{2+}$  containing six-, five-, and four-membered rings. These calculations correspond to the case of reasonably high flexibility of the zeolite lattice and reveal some common tendency of the  $\text{Zn}^{2+}$  ion stabilization in different rings.

## Results and Discussion

Calculated structures for the  $\text{Zn}^{2+}$  ion in six-, five-, and four-membered zeolitic rings are shown in Figures 2a, 4a, and 7a. They are labeled in Table 1 as structures **I**, **III**, and **VI**. Full geometry optimization for the  $\text{Zn}^{2+}$  ion in the six- and five-membered ring leads to a nearly planar structure (T atoms and Zn are in one plane) and to a pyramidal one for the four ring. The deformation of the six-membered ring because of the interaction of  $\text{Zn}^{2+}$  with four out of six oxygen atoms is remarkable (Figure 2a). Mulliken charges of Zn in six, five,

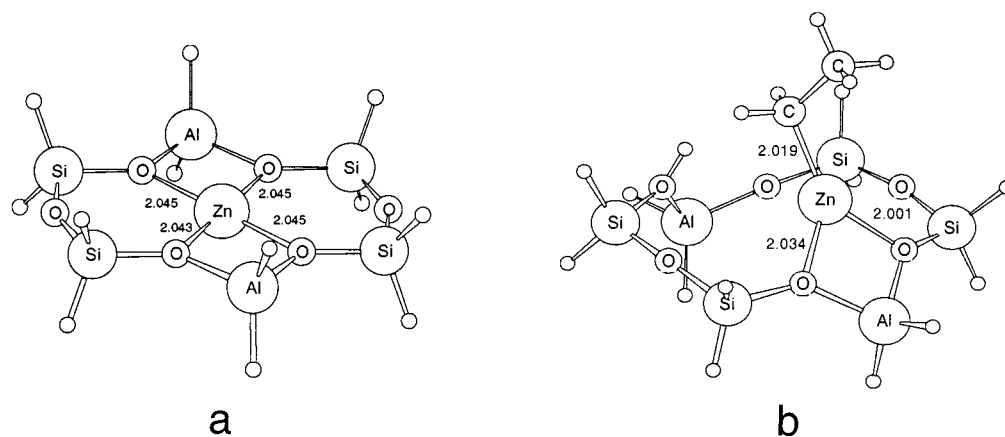


**Figure 2.** (A) Zn form of the six-ring cluster model with full geometry optimization; (B) decomposition of ethane on Zn form of the six-ring cluster model with full geometry optimization.

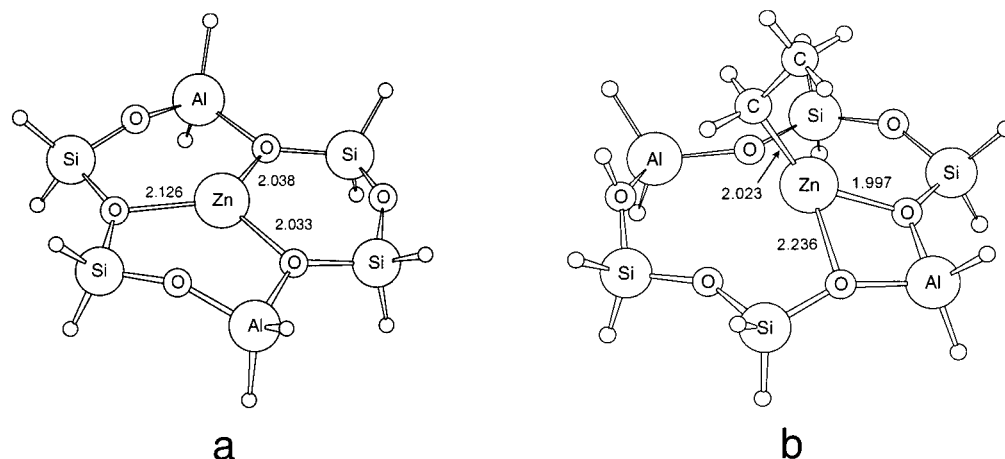


**Figure 3.** (A) Zn form of the six-ring cluster model with restricted geometry optimization; (B) decomposition of ethane on Zn form of the six-ring cluster model with restricted geometry optimization.

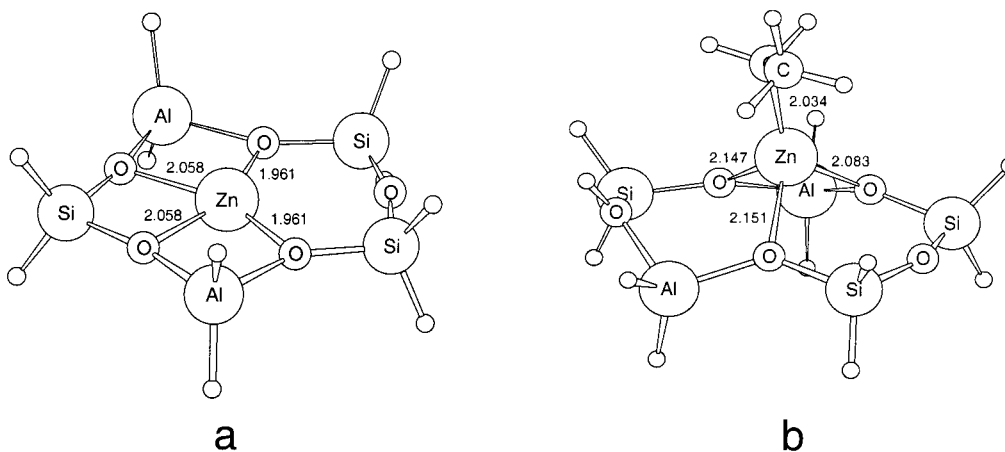


**Figure 4.** (A) Zn form of the five-ring cluster model with full geometry optimization; (B) decomposition of ethane on Zn form of the five-ring cluster model with full geometry optimization.

and four rings are +1.19, +1.13, +1.06 at DFT level. Charge distribution (also at DFT level) for a six-membered ring is as follows: Al(+0.97), Si(+1.12), and O<sub>1</sub>(−1.08) in the Al—O—Si bridge and O<sub>2</sub>(−0.96) in the Si—O—Si bridge. Differences in charges on Si, Al, and O for six and five rings are relatively small ( $\sim 0.02$ ). The polarization of the charge distribution slightly decreases in the four-membered ring in comparison with that in the six and five rings. Fully optimized geometries of the H forms of zeolite rings are substantially nonplanar, especially for the six-ring structure. Nevertheless, as shown by additional

computations with applied geometrical constrains (Si and Al are all in one plane), the difference in total energy between fully optimized and planar structures of the H form is quite small ( $\sim 4$  kcal/mol) at all levels of computation. It is interesting that exchange of  $\text{Zn}^{2+}$  by two protons does not cause drastic changes in the charges of Al, Si, and O in the ring, although the total charge on  $2\text{H}^+$  (+0.896) is somewhat smaller than on  $\text{Zn}^{2+}$  (+1.195). Comparison of the energies of the Zn and H forms of the rings shows that the reduction of  $\text{Zn}^{2+}/\text{Z}$  by  $\text{H}_2$  is a rather endothermic process. It was found that  $E_{\text{st}}$  substantially decreases



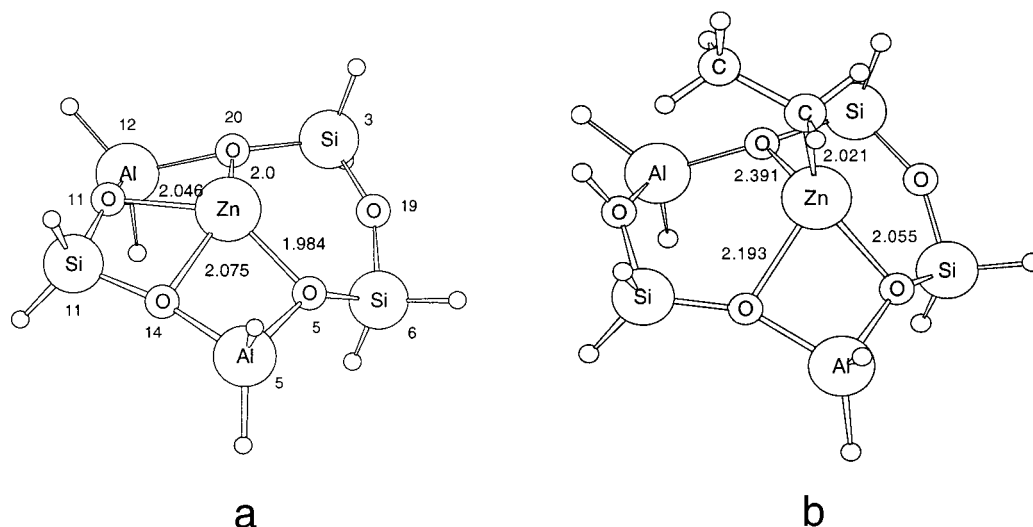


**Figure 5.** (A) Zn form of the five-ring cluster modeling five-membered ring in the straight channel of ZSM-5 (restricted geometry optimization); (B) decomposition of ethane on this five-ring cluster (restricted geometry optimization). Numbers at atoms correspond to crystallographic positions of ions in the ZSM-5 lattice structure.<sup>28</sup>

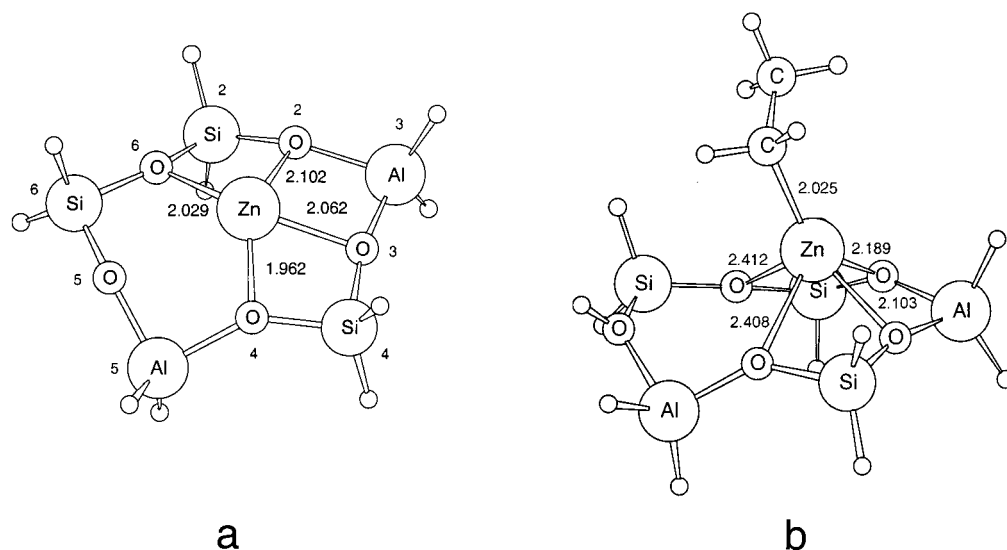


**Figure 6.** (A) Zn form of the five-ring cluster modeling five-membered ring in the sinusoidal channel of ZSM-5 (restricted geometry optimization); (B) decomposition of ethane on this five-ring cluster (restricted geometry optimization). Numbers at atoms correspond to crystallographic positions of ions in the ZSM-5 lattice structure.<sup>28</sup>

in the series six-, five-, and four-membered rings. The reason for differences in  $E_{st}$  for the discussed structures lies in substantially different possibilities for  $Zn^{2+}$  ion to form coordination bonds with oxygen ions of the six-, five-, and four-membered rings. This is manifested, for example, in the noticeably pyramidal complex structure of  $Zn^{2+}$  in a four-membered ring.  $Zn^{2+}$  is too big to fit in the four ring to form the preferable planar structure. The trend in  $E_{st}$  (see Table 1) is very important for understanding of the relative adsorption ability and catalytic activity of  $Zn^{2+}$  in cationic sites of different zeolites.

This was confirmed by calculations of the heterolytic dissociation of ethane on  $Zn^{2+}/Z$ . The reaction is endothermic: 46.5, 28.3, and 8.7 kcal/mol for the six, five, and four ring, respectively, at DFT level (see Table 1, structures **I**, **III**, and **VI**). In accordance with these calculations, probably only  $Zn^{2+}$  in the four-membered ring can be active in dehydrogenation of light alkanes.<sup>16</sup> The resulting structures of ethane dissociation on  $Zn^{2+}/Z$  are shown in Figures 2b, 4b, and 7b.

The calculated relative stability of different zeolite structures containing  $Zn^{2+}$  ions was used for qualitative analysis of two

different kinds of zeolites: faujasites (ZnHY) and high-silica zeolites (ZnHZSM-5).

**ZnHY Zeolites.** It is well-known that  $S_{II}$  (six-membered rings) and  $S_{III}$  sites (effective four-membered rings) are the only sites accessible for reagents in Y zeolites, but  $S_{III}$  sites have low occupation numbers by  $Zn^{2+}$  ions. This observation is in agreement with the calculated comparative stability of the  $Zn^{2+}$  ion in four and six rings. The most remarkable result of our calculations is the rather high stabilization energy  $E_{st}$  for the  $Zn^{2+}$  ion in the six ring both for the cluster model with full geometry optimization and for the model with imposed restrictions during the optimization ("realistic" zeolite model II; Figure 3a, see Table 1). This can explain the failure to observe the reduction of  $Zn^{2+}/Z$  by hydrogen in ZnHY zeolites<sup>29</sup> and the experimental data on zinc metal vapor deposition.<sup>30</sup> It has been suggested that the poor activity of the faujasites in dehydrogenation of light alkanes was the result of a low occupation of the  $S_{II}$  sites by  $Zn^{2+}$  ions if ion exchange was used.<sup>7</sup> As we have shown, it is more reasonable to associate the comparatively low chemical activity of Zn faujasites with high stability of  $Zn^{2+}$  in six-membered rings. This results in low activity of these sites

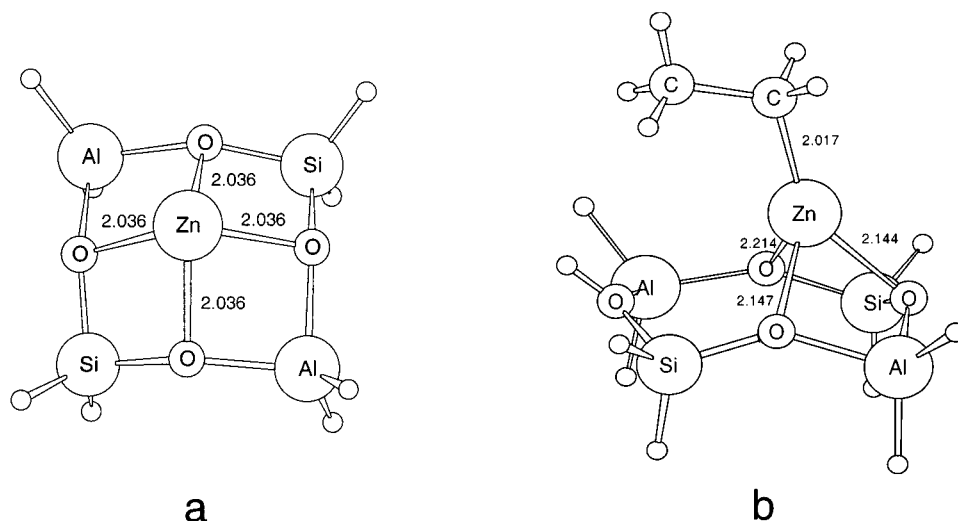


**Figure 7.** (A) Zn form of the four-ring cluster model with full geometry optimization; (B) decomposition of ethane on Zn form of the four-ring cluster model with full geometry optimization.

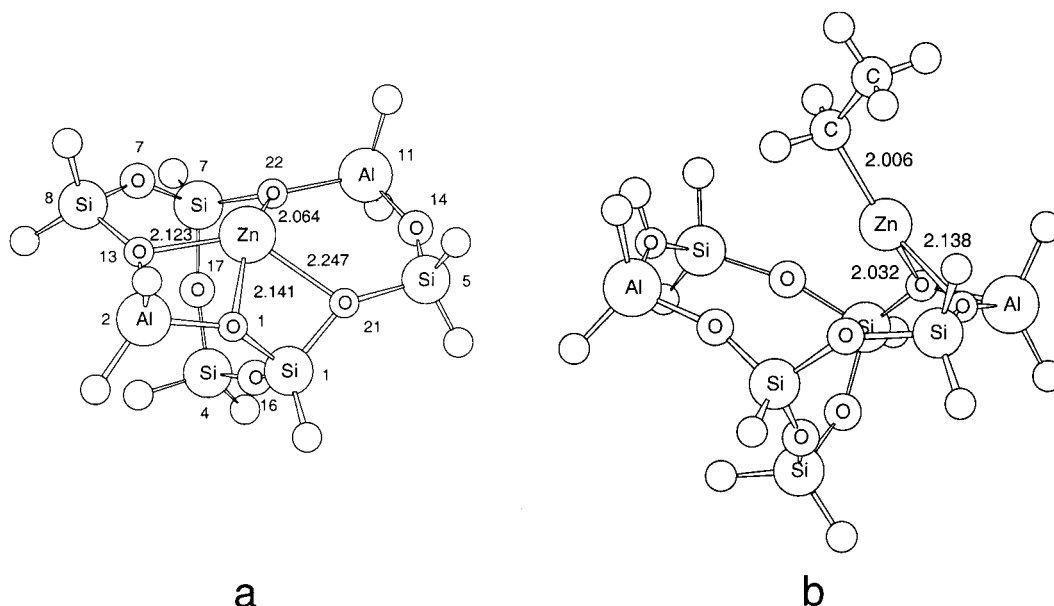
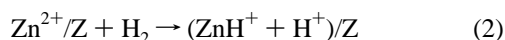


**Figure 8.** (A) Zn form of the  $\alpha$  site in ZSM-5 structure (restricted geometry optimization); (B) decomposition of ethane on this  $\alpha$  site (restricted geometry optimization). Numbers at atoms correspond to crystallographic positions of ions in the ZSM-5 lattice structure.<sup>28</sup>

in the heterolytic dissociation of hydrogen:



(see Table 1). This can also rationalize the fact that reaction 2 was not observed in ZnNaY zeolites prepared by ion exchange.<sup>10</sup>

We have also carried out calculations of the heterolytic dissociation of ethane as the first step of the dehydrogenation reaction. An “alkyl” route of the reaction<sup>17</sup> was considered:



The reaction is strongly endothermic. The calculated heat of the reaction is 46.5 kcal/mol at the DFT level (49.4 kcal/mol at HF level) for full geometry optimization and 37.5 kcal/mol for the restricted geometry optimization of the six-ring cluster (see Table 1). Remarkable changes in the structure of the site take place upon reaction 3. The  $\text{Zn}^{2+}$  ion goes out of the ring plane and decreases its coordination to the framework oxygen ions from 4 (Figure 2a) and 3 (Figure 3a) to 2 (Figures 2b and 3b). The charge (at DFT level) of the Zn ion decreases from +1.19

to +0.99 for structure **I** and from +1.17 to +0.97 for structure **II** (see Table 1) as a consequence of coordination of the alkyl group.

It is interesting to compare the “alkyl” route of reaction 3 with the “carbenium” one:



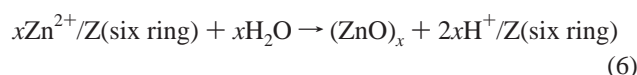
The latter is usually proposed in the catalytic literature.<sup>1,31</sup> For example, the calculated heat of reaction for the “carbenium” route is 52.4 kcal/mol at DFT level (54.7 kcal/mol at HF level) in the case of the six-ring cluster with full geometry optimization. The present results agree with those of Chep et al.<sup>18</sup> that the “alkyl” route is preferable; however, in our case, the difference is small (~5 kcal/mol if compared to the corresponding energies mentioned above).

An attempt to stabilize zinc oxide particles in ZnHY zeolites showed that these species are rather unstable and disappear during the dehydration of the zeolite (vacuum treatment at temperature above 300 °C).<sup>10</sup> This process is accompanied by a

decrease in the intensity of IR bands from the bridged hydroxyl group. Our calculations of the  $\text{Zn}^{2+}$  zeolite cationic sites allowed us to consider the question of the comparative stability of small oxide particles in zeolite cavities. First, note that the reduction of very small oxide species by hydrogen is a rather exothermic process. At our DFT level of calculation, the gain in energy for the exothermic reaction of ZnO molecules with hydrogen

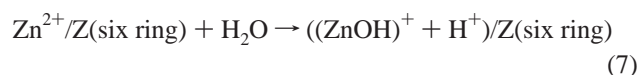


is 69.2 kcal/mol. Note that the increase of the size of oxide particles substantially decreases and even reverses the overall energy effect of this reaction. In particular, a calculation for the hypothetical cuban oxide structure of  $(\text{ZnO})_4$  gives only  $-8.9$  kcal/mol at DFT level. Nevertheless, it is evident that conditions for formation of oxide species  $(\text{ZnO})_n$  in faujasites are, as a rule, unfavorable. For example, for the faujasite-like structure **II**, the heat of the reaction (at DFT level)



is 142.1 and 64.0 kcal/mol per one  $\text{Zn}^{2+}$  ion for  $x = 1$  and 4, which corresponds to the formation of an isolated ZnO molecule and a cubic  $(\text{ZnO})_4$  cluster, respectively.

It is of interest that calculations of the interaction of  $\text{Zn}^{2+}/\text{Z}$  with a water molecule showed that the energy of molecular adsorption is quite significant. It is equal to 24.2 kcal/mol for structure **I** and 29.0 kcal/mol for structure **II** (at DFT level). This is in qualitative agreement with experimental data.<sup>24</sup> As for the reaction

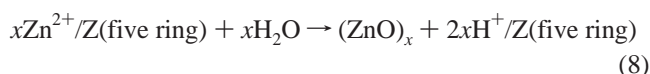


we were unable to find any structure corresponding to the heterolytic dissociation of water. Irrespective of the starting point, the optimization resulted, for both full and restricted optimization, in the molecular water adsorption.

**ZnHZSM-5.** Up to now there are uncertainties concerning the nature of the  $\text{Zn}^{2+}$  ion containing structures in ZnHZSM-5 zeolites. In principle, it should substantially depend on the Si/Al ratio and on the method of introducing zinc into the zeolite. Generally speaking, the following forms should be considered: (a)  $\text{Zn}^{2+}$  ions in the exchangeable cationic positions,<sup>3,5</sup> (b)  $\text{Zn}^{2+}$  ions in a “nest” of defect sites of the zeolite matrix,<sup>5</sup> (c) some bi- or polynuclear structures consisting of closely localized Zn ions in cation positions connected via oxygen bridge,<sup>3</sup> and (d) small extraframework  $(\text{ZnO})_n$  clusters in zeolite channels and cavities.<sup>13</sup> The above-mentioned cluster model of the five-membered ring seems to be reasonable for exchangeable cationic sites in ZSM-5, but the probability of close localization of two Al atoms in the lattice depends on the Si/Al ratio. The relative number of such sites strongly decreases as the Si/Al ratio increases. This kind of sites is represented in our calculations by model **III** (the cluster with full optimization of geometry) and by structures **IV** and **V** as models of “real” five-membered rings in the straight and sinusoidal ZSM-5 channels, respectively (see Figures 1, 5, and 6). The geometry of the latter two structures was optimized using the procedure described above. The results of calculation of  $E_{\text{st}}$  and the energy of ethane heterolytic dissociation are shown in Table 1. We can conclude that the peculiarities of the “real” geometry of zeolite rings taken into account in calculations substantially influence the stabilization energies of the  $\text{Zn}^{2+}$  ion at these sites and the reaction

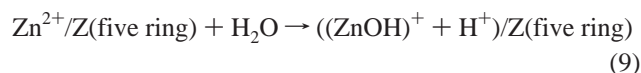
energies. To discuss the reactivity of these sites, one should compare the above-mentioned calculated energies with those for the  $\text{Zn}^{2+}$  ion in the four-membered ring (structure **VI**). It was shown earlier<sup>17</sup> that this site is active in the alkane dehydrogenation reaction. The comparison shows that stabilization of  $\text{Zn}^{2+}$  in five-membered rings is significantly stronger than in four-membered rings, which correlates with their activity in the ethane heterolytic dissociation. It is interesting that  $E_{\text{st}}$  and  $E_{\text{ads}}(\text{C}_2\text{H}_6)$  for  $\text{Zn}^{2+}$  in the  $\alpha$  site (structure **VII**, Figure 8) are quite similar to those obtained for the four-membered ring. The  $\alpha$  site was proposed as preferable structures for localization of polyvalent exchangeable cations in MFI systems.<sup>14</sup> In general, the energies of intermediates of ethane dehydrogenation are close for different sites considered in ZnZSM-5, and the largest differences are obtained for the first step of the reaction. Further discussion of the relative catalytic activity of  $\text{Zn}^{2+}$  in these sites relates to the question which reaction step is rate limiting and requires the calculation of activation barriers.

It is not surprising that the low stabilization energy for  $\text{Zn}^{2+}$  in ZSM-5 compared to that of the faujasites is favorable for formation of small zinc oxide clusters. For example, for structure **V**, the energy of the reaction



is 104.9 and 26.8 kcal/mol (at DFT level) per one  $\text{Zn}^{2+}$  ion for formation of isolated ZnO molecule or  $(\text{ZnO})_4$  cluster, respectively. Taking into account the stabilization of zinc oxide particles by zeolite lattice it could decrease these values further.

In contrast to faujasite, we have found structures corresponding to water heterolytic dissociation on all of the five-membered ring structures (**III–V**). The reaction



is exothermic with the energy gain (at DFT level) of 21.6 kcal/mol for structure **III**, 26.7 kcal/mol for structure **IV**, and 28.1 kcal/mol for structure **V**. This probably can explain why a fraction of Zn cations in the ZSM-5 structure is present in epy  $\text{ZnOH}^+$  form.<sup>5</sup> The reason we did not find water dissociation on  $\text{Zn}^{2+}$  for ZnHY zeolites is in the significantly larger  $\text{Zn}^{2+}$  stabilization energy in six rings of faujasite compared to five rings of ZSM-5.

## Conclusion

Ab initio cluster model calculations of comparative stabilization energies of  $\text{Zn}^{2+}$  in six-, five- and four-membered zeolite rings have been carried out. The stabilization energy was determined as the energy of the reaction with a hydrogen molecule resulting in the H form of the ring. Calculations with full geometry optimization of the clusters indicated quite large  $E_{\text{st}}$  for six- and five-membered rings with a significant decrease in the case of the four-membered ring. It was shown that different deformations of the rings could substantially decrease  $E_{\text{st}}$ . Such deformations can imitate some of the restrictions imposed by the crystal lattice in real systems and were introduced in the calculations by the specially frozen positions of boundary  $\text{H}^*$  atoms saturating the dangling bonds. It is important to take into account these peculiarities of the “real geometry” of the active sites for a proper understanding of their chemical activity. In accordance with our calculations, low activity of Zn-containing faujasites in alkane dehydrogenation

can be associated with high stabilization of  $\text{Zn}^{2+}$  ions in cationic  $\text{S}_{II}$  positions. Substantial decrease of the localization stability of  $\text{Zn}^{2+}$  in cationic positions formed by five- and especially four-membered rings in ZSM-5 zeolites make these systems much more reactive. Such a favorable destabilization of  $\text{Zn}^{2+}$  bonding can result from a steric hindrance, as in the case of four-membered rings, or can arise from a larger spatial separation of two  $\text{Al}^{3+}$  ions as in the structure of  $\alpha$  site. The latter site seems to be the most favorable for the localization of  $\text{Zn}^{2+}$  ions and is the good candidate as an active site for alkane dehydrogenation. Another consequence of lower stability of  $\text{Zn}^{2+}$  ions in cationic positions of ZSM-5 is an appearance of favorable conditions for the formation of small intrazeolite zinc oxide particles. These species as well as  $(\text{Zn}-\text{O}-\text{Zn})^{2+}$  structures can be important for the dehydrogenation ability of ZnZSM-5 zeolites. Our calculations have shown high activity of these particles in activation of alkanes.

**Acknowledgment.** The financial support from Dutch Science Foundation in the collaborative Russian–Dutch research project 047-005-011 NWO is gratefully acknowledged.

## References and Notes

- (1) Mole, T.; Anderson, J. R.; Creer, G. *Appl. Catal.* **1985**, *17*, 141.
- (2) Ono, Y. *Catal. Rev.—Sci. Eng.* **1992**, *34*, 179.
- (3) Biscardi, J. A.; Meitzner, G. D.; Iglesia, E. *J. Catal.* **1998**, *179*, 192.
- (4) Biscardi, J. A.; Iglesia, E. *Catal. Today* **1996**, *31*, 207.
- (5) El-Malki, El-M.; van Santen, R. A.; Sachtler, W. M. H. *J. Phys. Chem. B* **1999**, *103*, 4611.
- (6) Seidel, A.; Boddenberg, B. *Chem. Phys. Lett.* **1996**, *249*, 117.
- (7) Seidel, A.; Kampt, G.; Schmidt, A.; Boddenberg, B. *Catal. Lett.* **1998**, *51*, 213.
- (8) Dziewiecki, A.; Hydzik, P. *J. Appl. Chem.* **1996**, *40*, 27.
- (9) Zhao, X. S.; Lu, G. G.; Millar, G. J. *J. Porous Mater.* **1996**, *3*, 61.
- (10) Kazansky, V. B.; Borovkov, V. Yu.; Serykh, A. I.; van Santen, R. A.; Stobbelaar, P. J. *J. Phys. Chem. Chem. Phys.*, **1999**, *1*, 2881.
- (11) Herron, N.; Wang, Y.; Eddy, M. M.; Stucky, G. D.; Cox, D. E.; Moller, K.; Bein, T. *J. Am. Chem. Soc.* **1989**, *111*, 530.
- (12) Wark, M.; Kessler, H.; Schulz-Ekloff, G. *Microporous Mater.* **1997**, *8*, 241.
- (13) Kazansky, V. B.; Borovkov, V. Yu.; Serykh, A. I.; van Santen, R. A.; Anderson, B. *Catal. Lett.* **2000**, *66*, 39.
- (14) Wichterlova, B.; Dedeczek, J.; Sobalik, Z. In *Proceedings of the 12th International Zeolite Conference*, Baltimore, MD; Materials Research Society: Warrendale, PA, 1998; p 941.
- (15) Zhanpeisov, N. U.; Nakatsuji, H.; Hada, M.; Nakai, H.; Anpo, M. *Catal. Lett.* **1996**, *42*, 173.
- (16) Trout, B. L.; Chakraborty, A. K.; Bell, A. T. *J. Phys. Chem.* **1996**, *100*, 4173.
- (17) Frash, M. V.; van Santen, R. A. *J. Phys. Chem. Chem. Phys.* **2000**, *2*, 1085.
- (18) Chep, N. S.; Doyemet, J. Y.; Guisnet, M. *J. Mol. Catal.* **1988**, *45*, 281.
- (19) Becke, A. D. *J. Chem. Phys.* **1993**, *98*, 5648.
- (20) Perdew, J. P. *Phys. Rev. B* **1986**, *33*, 8822.
- (21) (a) Frisch, M. J.; Trucks, G. W.; Head-Gordon, M.; Gill, P. M. W.; Wong, M. W.; Foresman, J. B.; Johnson, B. G.; Schlegel, H. B.; Robb, M. A.; Replogle, E. S.; Gomperts, R.; Andres, J. L.; Rahavachari, K.; Binkley, J. S.; Gonzalez, C.; Martin, R. L.; Fox, D. J.; Defrees, D. J.; Baker, J.; Stewart, J. J. P.; Pople, J. A. *Gaussian 92*; Gaussian, Inc.: Pittsburgh, PA, 1992. (b) Frisch, M. J.; Trucks, G. W.; Schlegel, H. B.; Scuseria, G. E.; Robb, M. A.; Cheeseman, J. R.; Zakrzewski, V. G.; Montgomery, J. A., Jr.; Stratmann, R. E.; Burant, J. C.; Dapprich, S.; Millam, J. M.; Daniels, A. D.; Kudin, K. N.; Strain, M. C.; Farkas, O.; Tomasi, J.; Barone, V.; Cossi, M.; Cammi, R.; Mennucci, B.; Pomelli, C.; Adamo, C.; Clifford, S.; Ochterski, J.; Petersson, G. A.; Ayala, P. Y.; Cui, Q.; Morokuma, K.; Malick, D. K.; Rabuck, A. D.; Raghavachari, K.; Foresman, J. B.; Cioslowski, J.; Ortiz, J. V.; Stefanov, B. B.; Liu, G.; Liashenko, A.; Piskorz, P.; Komaromi, I.; Gomperts, R.; Martin, R. L.; Fox, D. J.; Keith, T.; Al-Laham, M. A.; Peng, C. Y.; Nanayakkara, A.; Gonzalez, C.; Challacombe, M.; Gill, P. M. W.; Johnson, B. G.; Chen, W.; Wong, M. W.; Andres, J. L.; Head-Gordon, M.; Replogle, E. S.; Pople, J. A. *Gaussian 98*; Gaussian, Inc.: Pittsburgh, PA, 1998.
- (22) Tatewaki, H.; Sakai, Y.; Huzinaga, S. *J. Comput. Chem.* **1982**, *2*, 278.
- (23) Ciruolo, M. F.; Norby, P.; Hanson, J. C.; Corbin, D. R.; Grey, C. P. *J. Phys. Chem. B* **1999**, *103*, 346.
- (24) McCusker, L. B.; Seff, K. *J. Phys. Chem.* **1981**, *85*, 405.
- (25) Khouchaf, L.; Tuilier, M.-H.; Wark, M.; Soular, M.; Kessler, H. *Microporous Mesoporous Mater.* **1998**, *20*, 27.
- (26) Pierloot, K.; Delabie, A.; Ribbing, C.; Verberckmoes, An. A.; Schoonheydt, R. A. *J. Phys. Chem. B* **1998**, *102*, 10789.
- (27) Olson, D. H. *J. Phys. Chem.* **1979**, *74*, 2758.
- (28) Lermer, H.; Draeger, M.; Steffen, J.; Unger, K. K. *Zeolites* **1985**, *5*, 131.
- (29) Berndt, H.; Lietz, G.; Voelter, J. *J. Appl. Catal. A: General* **1996**, *146*, 365.
- (30) Seidel, A.; Rittinger, F.; Boddenberg, B. *J. Phys. Chem. B* **1998**, *102*, 7176.
- (31) Derouane, E. G.; He, H.; Derouane-Abd Hamid, S. B.; Ivanova, I. *Catal. Lett.* **1999**, *58*, 1.